# Functionalization of liquid-exfoliated two-dimensional 2H-MoS$_2$

Claudia Backes,[a,c] Nina C. Berner,[a,b] Xin Chen,[a,b] Paul Lafargue,[a,b] Pierre LaPlace,[a,b] Mark Freeley,[a,b] Georg S. Duesberg,[a,b] Jonathan N. Coleman,[a,c] and Aidan R. McDonald*[a,b]

**Abstract:** The study of layered two-dimensional (2D) inorganic transition metal dichalchogenides (TMDs) has attracted great interest due to their potential application in optoelectronics, catalysis, and medicine. However, methods to functionalize and process such 2D TMDs remain scarce. We have established a facile route towards functionalized layered molybdenum disulfide (MoS$_2$). We found that the reaction of liquid-exfoliated 2D MoS$_2$ with M(OAc)$_2$ salts (M = Ni, Cu, Zn; OAc = acetate) yielded functionalized MoS$_2$-M(OAc)$_2$. Importantly, this has furnished the 2H-polytype of MoS$_2$, which is semiconducting. X-ray photoelectron spectroscopy (XPS) analysis supports coordination of surface S-atoms to the M(OAc)$_2$, as evidenced by the appearance of new S 2p features in the XPS core level spectra of the functionalized materials. Diffuse reflectance infrared Fourier transform (DRIFT-IR) and thermogravimetric analysis (TGA) also provide strong evidence for the presence of carboxylate moieties on the 2H-MoS$_2$. Most interestingly, functionalization of the 2H-MoS$_2$ allows for its dispersion/processing in more conventional lab solvents.

The study of the layered two-dimensional (2D) inorganic transition metal dichalchogenides (TMDs) has recently received growing attention.[1] This is mainly due to their potential in applications ranging from optoelectronics, catalysis, electrochemistry and medicine.[1-2] While significant progress has been made on the production of ultra-thin, high quality TMDs by chemical vapor deposition (CVD) growth,[3] chemical exfoliation,[1b, 4] or direct exfoliation in suitable solvents,[1c, 5] reports on the functionalization of 2D TMDs remain scarce, limiting their further application. Functionalization of nanomaterials is critical for, amongst others, tailoring their surface properties to specific solvents/environments, enhancing their processability, and modulating their conductivity. Even though 2D TMDs show good dispersibility in certain solvents, such as *N*-methyl-2-pyrrolidone (NMP), their dispersibility and thus processability falls short in common lab solvents. To date TMDs have proven difficult to functionalize because of their relative inertness. We set out to investigate a route towards functionalized TMDs, with the goals of understanding how to prepare such functionalized materials and identify methods to enhance their solution processability.

As a model 2D TMD, we have focused our attention on MoS$_2$. We have recently reported methods for the facile preparation and extensive characterization of exfoliated MoS$_2$.[5-6] 2D MoS$_2$ has primarily been isolated in two polytypes, 2H- and 1T-MoS$_2$.[1b] In 2H-MoS$_2$ the Mo-atom sits in a trigonal planar environment, whereas in 1T-MoS$_2$ the Mo-atom sits in an octahedral environment. Critically, the polytypes display disparate electronic properties: 2H-MoS$_2$ is a semi-conductor, whereas 1T-MoS$_2$ is metallic.[4, 7] While, a number of reports describing the covalent functionalization of MoS$_2$ have recently appeared,[8] all have employed a three-step procedure that ultimately yields functionalized 1T-MoS$_2$.[4] To the best of our knowledge, no methods for the functionalization of pristine 2D 2H-MoS$_2$ exist, and thus there remains no access to functionalized 2D TMD semi-conductors at present. Herein we report methods for the facile functionalization of layered 2H-MoS$_2$.
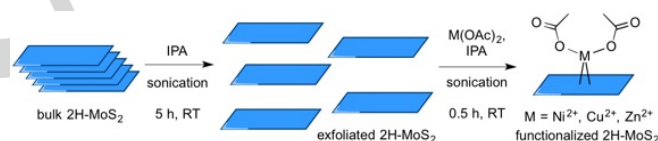


**Figure 1.** Schematic representation of the procedure for exfoliation and functionalization of 2H-MoS$_2$ nanosheets (IPA = 2-propanol, M(OAc)$_2$ = metal acetate salts).

In order to functionalize 2H-MoS$_2$ in a mild and efficient manner, we have employed similar liquid exfoliation techniques to those reported recently.[1c, 5-6, 6d, 9] Rather than using the standard dispersion/exfoliation solvents employed previously, however, we used 2-propanol (IPA). Typically for 2H-MoS$_2$ exfoliation, NMP and *N*-cyclohexyl-2-pyrrolidone (CHP) are used due to the matching solubility parameters of solvent and solute.[1c, 5, 9b, 9] We found these solvents unsuitable because: they tend to leave a residue on the surface of the 2H-MoS$_2$ that inhibited functionalization; their high boiling point prevented efficient drying and characterization of the functionalized material; NMP has been identified as a reproductive toxin. Prior to functionalization, commercially available 2H-MoS$_2$ was initially sonicated in IPA for 5 h (see supporting information). Subsequent isolation of the exfoliated 2H-MoS$_2$ was achieved by centrifugation to remove unexfoliated material. As evidenced by atomic force microscopy (AFM, Figure 2), the 2H-MoS$_2$ has been successfully exfoliated in IPA. AFM length and thickness analysis on a number of nanosheets was used to determine the mean lateral dimension <L> (260 nm) and degree of exfoliation <N> (9-10 layers) of the IPA-exfoliated 2H-MoS$_2$. Even though the concentration of exfoliated 2H-MoS$_2$ was typically lower by a factor of three compared to NMP,[5] IPA was found to be a suitable solvent, eliminating the problems associated with NMP/CHP.

[a]    Dr. Claudia Backes, Dr. Nina C. Berner, Xin Chen, Paul Lafargue, Pierre LaPlace, Mark Freeley, Prof. Georg S. Duesberg, Prof. Jonathan N. Coleman, Dr. Aidan R. McDonald
       CRANN/AMBER Nanoscience Institute, Trinity College Dublin (TCD), College Green, Dublin 2, Ireland
       E-mail: aidan.mcdonald@tcd.ie
[b]    School of Chemistry, TCD
[c]    School of Physics, TCD

       Supporting information for this article is given via a link at the end of the document.
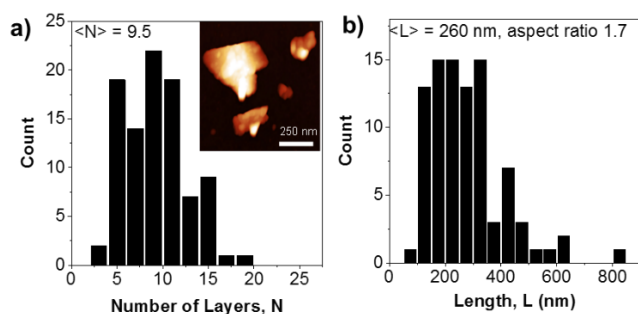
**Figure 2.** Atomic force microscopy after drop-casting a 2H-MoS$_2$ dispersion on Si/SiO$_2$ wafers (image in inset) (a) thickness histograms (b) length histogram.

The IPA-exfoliated 2H-MoS$_2$ was reacted with a variety of metal-acetate salts. We postulated that surface S-atoms of the exfoliated 2H-MoS$_2$ would coordinate to the metal-acetate salts, providing a facile route to functionalized 2H-MoS$_2$. The metal cations were anticipated to act as an anchor for (functional) organic carboxylate ligands to bind, altering the surface properties of the 2D 2H-MoS$_2$. Tremel and co-workers have taken a similar approach for the functionalization of TMD nanoparticles.[10] M(OAc)$_2$ salts (M = Cu, Ni, Zn) were dissolved in IPA (10 mM) and subsequently reacted with IPA-exfoliated 2H-MoS$_2$ (~0.2 mM, v/v = 1) under sonication for 30 min. M(OAc)$_2$ salts were identified as suitable functionalities for two reasons: they display solubility in a variety of common lab solvents (acetone, alcohols, nitriles, metal halides do not display such favorable solvation); they represent a large cohort of metal-carboxylate salts, where the carboxylate ligand can be easily changed allowing a broad scope of functional carboxylate group be tethered to the 2H-MoS$_2$ surface. A first indication of successful functionalization was provided through analysis of the optical extinction spectra of the functionalized materials. Upon functionalization we noted marked changes in the concentration of 2H-MoS$_2$ dispersed in the IPA reaction mixture (as evidenced by changes in optical extinction intensity), indicating the dispersion properties of the 2H-MoS$_2$ had been altered. For 2H-MoS$_2$-Cu(OAc)$_2$ and 2H-MoS$_2$-Zn(OAc)$_2$ the concentration of dispersed 2H-MoS$_2$ decreased over 48 h, suggesting partial reaggregation of the layered material. In contrast, 2H-MoS$_2$-Ni(OAc)$_2$ did not display any reaggregation of exfoliated 2H-MoS$_2$, and in fact yielded more stable 2H-MoS$_2$ dispersions than the parent unfunctionalized materials (Figure S1).

Critically, functionalization caused no changes in the relative intensities or energies of optical excitation features attributed to exfoliated 2H-MoS$_2$. This is very important, as it establishes that functionalization did not yield the 1T-polytype (1T-MoS2 has an extinction spectrum very distinct from 2H-MoS$_2$).[4, 6d] All other functionalization techniques to date have yielded 1T-MoS$_2$.[4, 8]

Further proof of successful functionalization was obtained through analysis of the post-reaction supernatant solutions (where all functionalized 2H-MoS$_2$ has been removed). Cu(OAc)$_2$ displays a unique electronic absorption handle ($\lambda_{max}$ = 700 nm) allowing us to monitor the uptake of the Cu$^{2+}$ salt by exfoliated 2H-MoS$_2$. A significant decrease in the $\lambda_{max}$ = 700 nm

feature assigned to Cu(OAc)$_2$ after functionalization was observed in the supernatant solutions, providing further strong evidence of uptake of M(OAc)$_2$ salts by 2H-MoS$_2$. In summary optical extinction spectroscopy provides encouraging evidence that functionalization of 2H-MoS$_2$ can be achieved through simple coordination chemistry techniques.
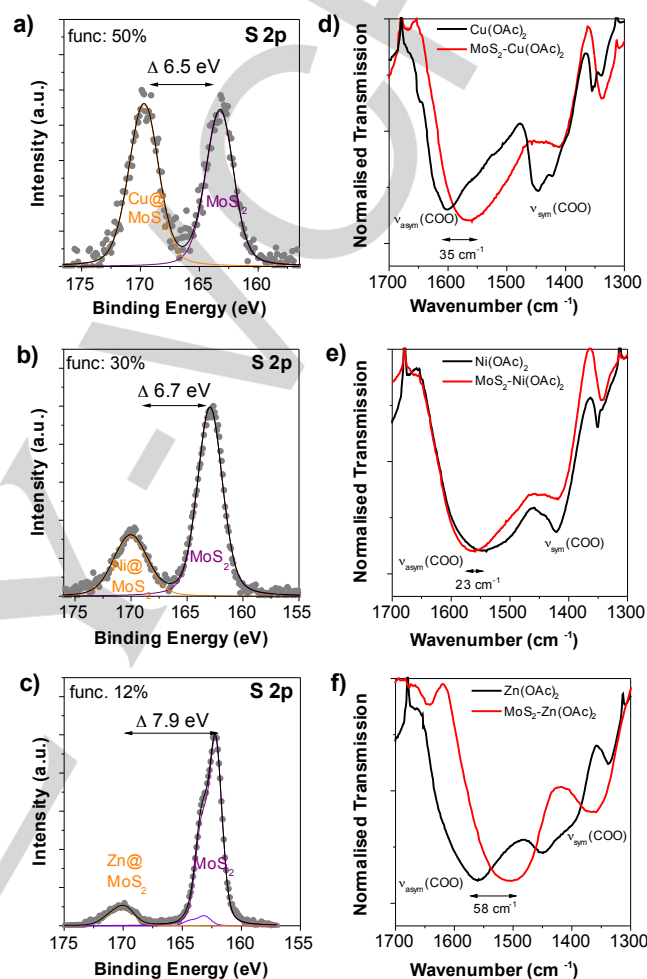


**Figure 3.** Left: Fitted XPS S 2p core level spectra[11] of the 2H-MoS$_2$-M(OAc)$_2$: M = a) Cu; b) Ni; c) Zn. Right: DRIFT spectra of the M(OAc)$_2$ salts and 2H-MoS$_2$-M(OAc)$_2$: M = d) Cu; e) Ni; f) Zn.

Unequivocal evidence for the coordination of surface 2H-MoS$_2$ S-atoms to the metal atoms of the M(OAc)$_2$ salts was obtained through X-ray photoelectron spectroscopy (XPS). Survey spectra (Table S1) of the material confirmed the presence of surface Mo, S, M (Cu, Ni, Zn), C, and O atoms consistent with the functionalization of 2H-MoS$_2$ by M(OAc)$_2$ salts. Significantly, in all fitted XPS S 2p core level spectra (Figures 3 and S3) a second well-separated component in the S 2p core level spectra at higher binding energies was clearly discernible in the functionalized materials. This is consistent with a proportion of surface S-atoms being found in a different chemical environment compared to the unfunctionalized material (Figure S3). As a result of coordination to the Lewis acidic metal atoms, the surface S-atom donors become more electropositive, resulting in

a higher photoelectron emission energy. Analysis of the same spectra allowed us to estimate the degree of functionalization of the 2H-MoS$_2$ surface (see supporting information). The ratio of the integrated peak intensity of the high-energy (coordinating) S 2p component to the total integrated S 2p core level peak yields a degree of surface functionalization of 50% in the case of 2H-MoS$_2$-Cu(OAc)$_2$, i.e. 50% of the S atoms on the surface bear a functional group. For 2H-MoS$_2$-Ni(OAc)$_2$, and 2H-MoS$_2$-Zn(OAc)$_2$ values of 30% and 10% high-energy S 2p component, respectively, were determined. This pronounced difference in the degree of functionalization is not unexpected. The binding affinity of Cu, Ni, and Zn towards thioether ligands (analogous to S-donors of 2H-MoS$_2$) tends to follow the trend Cu >> Ni > Zn.[12] We note that the successful chemical functionalization is also reflected in the Mo 3d core level XPS spectra (Figure S2). However, these spectra are too complex to provide clear insights into the functionalized 2H-MoS$_2$. Nonetheless, XPS analysis has allowed us to clearly establish a direct sulfur-metal interaction in exfoliated 2H-MoS$_2$-M(OAc)$_2$ nanomaterials.

The high degree of functionalization clearly demonstrates that the M(OAc)$_2$ functionalities are binding to the basal-plane of the 2D 2H-MoS$_2$. If the M(OAc)$_2$ functionalities were reacting only at disulfide-rich edge-sites,[13] the degree of functionalization would be expected to be considerably lower. We can estimate the ratio of edge to basal plane sites by modeling the 2H-MoS$_2$ nanosheets as rectangles with mean length of 260 nm and mean width of 150 nm (as determined from AFM, Figure 1). The perimeter (edge sites, 820 nm x 1 nm) constitutes roughly 2% of the sites that are present in the basal plane (39,000 nm$^2$) consequently yielding a maximum degree of edge-functionalization of 2%. This is an encouraging outcome, given that analysis of the XPS-determined values for the degree of surface functionalization would suggest that 50% of surface S-atoms in 2H-MoS$_2$-Cu(OAc)$_2$ coordinates to a Cu-atom.

To understand further the 2H-MoS$_2$-M(OAc)$_2$ interaction, we employed diffuse reflectance infrared Fourier transform (DRIFT) spectroscopy, which provided proof of a direct 2H-MoS$_2$/M(OAc)$_2$ interaction (Figures 3 and S4). The sharp feature observed at 383 cm$^{-1}$ is typical of 2H-MoS$_2$.[14] For all of the functionalized materials, the presence of the acetate ligands is clearly evidenced by the characteristic $\nu_{C=O}$ (1550-1600 cm$^{-1}$) of the metal-bound acetate ligand.[15] Significantly, in the functionalized materials, the $\nu_{C=O}$ associated with the acetate ligands are shifted by between 20 and 60 cm$^{-1}$ when compared to the parent M(OAc)$_2$ salts. This shift provides a strong indication of a change to the coordination environment at the metal center of the acetate salt, presumably as a result of ligation by the S-donors of the 2H-MoS$_2$ to the metal ion. 2H-MoS$_2$-Cu(OAc)$_2$ provides further revealing insights. In the solid state, Cu(OAc)$_2$ is a dimeric species containing two Cu atoms bridged by four acetate ligands ([Cu$_2$(OAc)$_4$]). The $\nu_{C=O}$ in 2H-MoS$_2$-Cu(OAc)$_2$ (1565 cm$^{-1}$) is typical of a species containing end-on binding (and not bridging (~1600 cm$^{-1}$)) acetate ligands.[16] These observations suggest the metal has been ligated by surface S-atoms causing the break-up of the dimeric [Cu$_2$(OAc)$_4$] resulting in the formation of 2H-MoS$_2$-Cu(OAc)$_2$ with monodentate end-on binding acetate ligands. In summary, the

pronounced shifts of the $\nu_{C=O}$ of the metal-bound acetate ligands strongly suggests an interaction between the metal centers and the sulfur atoms of the 2H-MoS$_2$.

Thermo-gravimetric analysis (TGA) provided further proof of successful functionalization of 2H-MoS$_2$. Between 50 °C and 400 °C, the parent 2H-MoS$_2$ displayed negligible weight loss. In contrast 2H-MoS$_2$-Cu(OAc)$_2$ displayed a significant (15%) and very sharp weight-loss at ~200 °C, indicative of the loss of organic surface functionalities (Figure S5). In support of this, DRIFT-IR analysis of the post-TGA 2H-MoS$_2$-Cu(OAc)$_2$ sample showed the disappearance of all $\nu_{C=O}$ features that were attributed to surface-bound acetate groups (Figure S6). This would suggest that the weight-loss at ~200 °C is as a result of the thermal decomposition of the organic surface groups.

An important aspect to the functionalization of 2D nanomaterials is the alteration of the surface properties of the material as a result of the attachment of functional moieties.[6a] To investigate the effects of the surface functionalities in 2H-MoS$_2$-M(OAc)$_2$, we have redispersed 2H-MoS$_2$-Cu(OAc)$_2$ in NMP, IPA and acetone. We have used 2H-MoS$_2$-Cu(OAc)$_2$ because it showed the highest degree of functionalization. We compared the dispersibility of 2H-MoS$_2$-Cu(OAc)$_2$ to an exfoliated 2H-MoS$_2$ reference material (Figure 4). The 2H-MoS$_2$ reference was dispersed well in NMP and showed a reasonable dispersibility in IPA. In acetone, no 2H-MoS$_2$ was stably dispersed. In contrast, the functionalized 2H-MoS$_2$-Cu(OAc)$_2$ could not be stably dispersed in NMP, was reasonably well dispersed in IPA, and displayed a significantly enhanced uptake in acetone.
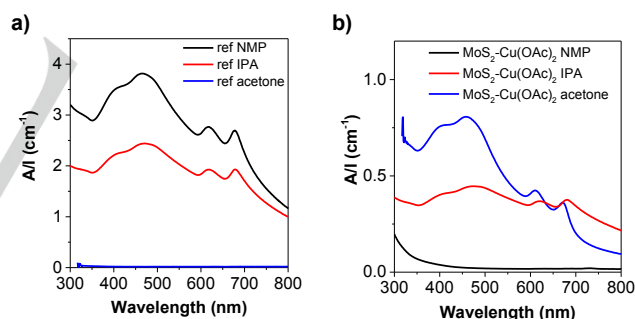


**Figure 4.** Optical extinction spectra after redispersion in NMP, IPA and acetone of pre-sonicated 2H-MoS$_2$ reference powder (a) compared to 2H-MoS$_2$-Cu(OAc)$_2$ (b).

Nanomaterial dispersibility can be described reasonably well in the framework of Hansen solubility parameters.[5, 17] To minimize the energetic cost of dispersion/solubilization, the enthalpy of mixing needs to be minimized. This is the case when solubility parameters ($\delta_D$, $\delta_P$, $\delta_{H,}$) of solvent and solute match (see supporting information).[5, 17] Using HSPiP (Hansen solubility parameters in practice, Y-MB algorithm) software, we can estimate the solubility parameters of the acetate ligands to be $\delta_D$ = 14.7 MPa$^{1/2}$, $\delta_P$ = 12.5 MPa$^{1/2}$, $\delta_H$ = 7.9 MPa$^{1/2}$. While polar and H-bonding Hansen solubility parameters are close to NMP, the dispersive component is significantly lower. It is thus expected that successful surface modification by functionalization

decreases the dispersibility in NMP. In our redispersion experiments, we show that this is indeed the case, as the concentration of '2H-MoS$_2$' (estimated from the extinction at 345 nm)[12] is reduced by a factor of > 40 in the 2H-MoS$_2$-Cu(OAc)$_2$ compared to the pristine 2H-MoS$_2$. In IPA ($\delta_D$ = 15.8 MPa$^{1/2}$, $\delta_P$ = 6.1 MPa$^{1/2}$, $\delta_H$ = 16.4 MPa$^{1/2}$), the concentration 2H-MoS$_2$-Cu(OAc)$_2$ is lower by a factor of 5 compared to the reference. This is consistent with destabilization of the dispersed 2H-MoS$_2$ after functionalization (Figure S1). However, as the solubility parameters of IPA neither perfectly match the acetate ligands, nor the 2H-MoS$_2$, quantitative analysis of this behavior is challenging. All three solubility parameters of the acetate ligands are close to acetone ($\delta_D$ = 15.5 MPa$^{1/2}$, $\delta_P$ = 10.4 MPa$^{1/2}$, $\delta_H$ = 7 MPa$^{1/2}$) so that an enhanced dispersibility of the functionalized 2H-MoS$_2$ is expected. From our optical extinction spectra, we observe a 20-fold increase in concentration of the functionalized 2H-MoS$_2$ in acetone compared to the non-functionalized 2H-MoS$_2$ – perfectly consistent with the expectation from Hansen solubility parameters. Overall, the introduction of M(OAc)$_2$ functionalities to the surface of exfoliated 2H-MoS$_2$ has dramatically altered the dispersibility properties of the material, allowing for the surface tuning of the material to specific solvents.

In conclusion, we have demonstrated a facile route towards functionalized 2H-MoS$_2$. Until now, protocols for the preparation of functionalized exfoliated TMDs like MoS$_2$ have yielded the 1T polytype, which is metallic. We have shown that the reaction of liquid exfoliated 2H-MoS$_2$ (a semiconductor) with metal-carboxylate salts yields functionalized 2H-MoS$_2$-M(OAc)$_2$. Functionalization was achieved through coordination of surface S-atoms with the metal center of the metal-carboxylate salts. XPS, DRIFT-IR, and TGA analysis provide strong support for this. Most interestingly, functionalization of the 2H-MoS$_2$ allows for its dispersion in non-conventional solvents including IPA and acetone. At present we are investigating a variety of copper(II) salts as functional groups on the surface of 2H-MoS$_2$. We expect to be able to disperse 2H-MoS$_2$ in solvents displaying a wide range of polarities (i.e. from water to aliphatic hydrocarbons).

## Acknowledgements

[1] (a) S. Z. Butler, S. M. Hollen, L. Cao, Y. Cui, J. A. Gupta, H. R. Gutierrez, T. F. Heinz, S. S. Hong, J. Huang, A. F. Ismach, E. Johnston-Halperin, M. Kuno, V. V. Plashnitsa, R. D. Robinson, R. S. Ruoff, S. Salahuddin, J. Shan, L. Shi, M. G. Spencer, M. Terrones, W. Windl, J. E. Goldberger, *ACS Nano* **2013**, *7*, 2898-2926; (b) M. Chhowalla, H. S. Shin, G. Eda, L.-J. Li, K. P. Loh, H. Zhang, *Nature Chem.* **2013**, *5*, 263-275; (c) V. Nicolosi, M. Chhowalla, M. G.

Kanatzidis, M. S. Strano, J. N. Coleman, *Science* **2013**, *340*, 1420; (d) M. Xu, T. Liang, M. Shi, H. Chen, *Chem. Rev.* **2013**, *113*, 3766–3798.

[2] Q. H. Wang, K. Kalantar-Zadeh, A. Kis, J. N. Coleman, M. S. Strano, *Nature Nanotech.* **2012**, *7*, 699-712.

[3] (a) Y. J. Zhan, Z. Liu, S. Najmaei, P. M. Ajayan, J. Lou, *Small* **2012**, *8*, 966-971; (b) A. Berkdemir, H. R. Gutierrez, A. R. Botello-Mendez, N. Perea-Lopez, A. L. Elias, C.-I. Chia, B. Wang, V. H. Crespi, F. Lopez-Urias, J.-C. Charlier, H. Terrones, M. Terrones, *Sci. Rep.* **2013**, *3*.

[4] G. Eda, H. Yamaguchi, D. Voiry, T. Fujita, M. Chen, M. Chhowalla, *Nano Lett.* **2011**, *11*, 5111-5116.

[5] J. N. Coleman, M. Lotya, A. O'Neill, S. D. Bergin, P. J. King, U. Khan, K. Young, A. Gaucher, S. De, R. J. Smith, I. V. Shvets, S. K. Arora, G. Stanton, H.-Y. Kim, K. Lee, G. T. Kim, G. S. Duesberg, T. Hallam, J. J. Boland, J. J. Wang, J. F. Donegan, J. C. Grunlan, G. Moriarty, A. Shmeliov, R. J. Nicholls, J. M. Perkins, E. M. Grieveson, K. Theuwissen, D. W. McComb, P. D. Nellist, V. Nicolosi, *Science* **2011**, *331*, 568-571.

[6] (a) G. Cunningham, M. Lotya, C. S. Cucinotta, S. Sanvito, S. D. Bergin, R. Menzel, M. S. P. Shaffer, J. N. Coleman, *ACS Nano* **2012**, *6*, 3468-3480; (b) A. O'Neill, U. Khan, J. N. Coleman, *Chem. Mater.* **2012**, *24*, 2414-2421; (c) K. R. Paton, E. Varrla, C. Backes, R. J. Smith, U. Khan, A. O'Neill, C. Boland, M. Lotya, O. M. Istrate, P. King, T. Higgins, S. Barwich, P. May, P. Puczkarski, I. Ahmed, M. Moebius, H. Pettersson, E. Long, J. Coelho, S. E. O'Brien, E. K. McGuire, B. M. Sanchez, G. S. Duesberg, N. McEvoy, T. J. Pennycook, C. Downing, A. Crossley, V. Nicolosi, J. N. Coleman, *Nature Mater.* **2014**, *13*, 624-630; (d) C. Backes, R. J. Smith, N. McEvoy, N. C. Berner, D. McCloskey, H. C. Nerl, A. O'Neill, P. J. King, T. Higgins, D. Hanlon, N. Scheuschner, J. Maultzsch, L. Houben, G. S. Duesberg, J. F. Donegan, V. Nicolosi, J. N. Coleman, *Nature Commun.* **2014**, *8*, 4576.

[7] (a) F. Wypych, R. Schollhorn, *Chem. Commun.* **1992**, 1386-1388; (b) E. Benavente, M. A. Santa Ana, F. Mendizábal, G. González, *Coord. Chem. Rev.* **2002**, *224*, 87-109.

[8] (a) S.-D. Jiang, G. Tang, Z.-M. Bai, Y.-Y. Wang, Y. Hu, L. Song, *RSC Adv.* **2014**, *4*, 3253-3262; (b) S. S. Chou, M. De, J. Kim, S. Byun, C. Dykstra, J. Yu, J. Huang, V. P. Dravid, *J. Am. Chem. Soc.* **2013**, *135*, 4584–4587; (c) L. Zhou, B. He, Y. Yang, Y. He, *RSC Adv.* **2014**, *4*, 32570-32578.

[9] (a) Y. Hernandez, M. Lotya, D. Rickard, S. D. Bergin, J. N. Coleman, *Langmuir* **2010**, *26*, 3208-3213; (b) S. Barwich, U. Khan, J. N. Coleman, *J. Phys. Chem. C* **2013**, *117*, 19212–19218; (c) J. N. Coleman, *Acc. Chem. Res.* **2013**, *46*, 14-22; (d) D. Hanlon, C. Backes, T. M. Higgins, M. Hughes, A. O'Neill, P. King, N. McEvoy, G. S. Duesberg, B. Mendoza Sanchez, H. Pettersson, V. Nicolosi, J. N. Coleman, *Chem. Mater.* **2014**, *26*, 1751-1763.

[10] M. N. Tahir, N. Zink, M. Eberhardt, H. A. Therese, U. Kolb, P. Theato, W. Tremel, *Angew. Chem. Int. Ed.* **2006**, *45*, 4809-4815.

[11] The S component centered at 163 eV is attributed to S at edges of the nano-sheets, see ref. 6d.

[12] K. Zhou, J. Liu, P. Wen, Y. Hu, Z. Gui, *Appl. Surf. Sci.* **2014**, *316*, 237-244.

[13] (a) J. V. Lauritsen, M. V. Bollinger, E. Lægsgaard, K. W. Jacobsen, J. K. Nørskov, B. S. Clausen, H. Topsøe, F. Besenbacher, *J. Catal.* **2004**, *221*, 510-522; (b) J. V. Lauritsen, J. Kibsgaard, S. Helveg, H. Topsoe, B. S. Clausen, E. Laegsgaard, F. Besenbacher, *Nature Nanotech.* **2007**, *2*, 53-58; (c) H. I. Karunadasa, E. Montalvo, Y. Sun, M. Majda, J. R. Long, C. J. Chang, *Science* **2012**, *335*, 698-702.

[14] T. J. Wieting, J. L. Verble, *Phys. Rev. B* **1971**, *3*, 4286-4292.

[15] Y. Mathey, D. R. Greig, D. F. Shriver, *Inorg. Chem.* **1982**, *21*, 3409-3413.

[16] G. B. Deacon, R. J. Phillips, *Coord. Chem. Rev.* **1980**, *33*, 227-250.

[17] (a) J. N. Coleman, *Adv. Func. Mater.* **2009**, *19*, 3680-3695; bJ. M. Hughes, D. Aherne, J. N. Coleman, *J. Appl. Pol. Sci.* **2013**, *127*, 4483-4491.

**Entry for the Table of Contents** (Please choose one layout)

## COMMUNICATION

Functionalization of liquid-exfoliated, defect-free, layered 2H-MoS$_2$ was achieved through coordination of metal carboxylate salts by basal plane S-atoms. The surface coordinated metal-centre acts as an anchor for ligating organic functionalities.

bulk 2H-MoS$_2$

1. Exfoliation
2. Functionalization

Functionalized 2H-MoS$_2$
M = Ni$^{2+}$, Cu$^{2+}$, Zn$^{2+}$

S 2p
MoS$_2$
170  165  160  155
**Binding Energy (eV)**

S 2p
Cu@ MoS$_2$
MoS$_2$
175  170  165  160
**Binding Energy (eV)**
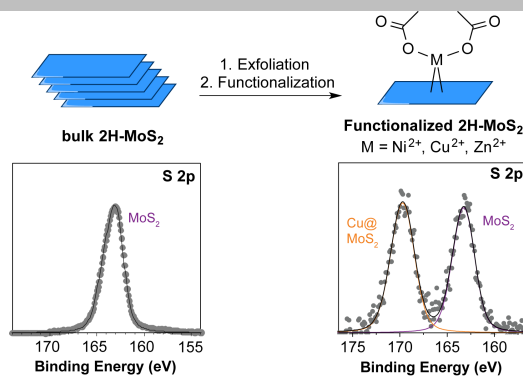
*Claudia Backes, Nina C. Berner, Xin Chen, Paul Lafargue, Pierre LaPlace, Mark Freeley, Georg S. Duesberg, Jonathan N. Coleman, and Aidan R. McDonald\**

**Functionalization of liquid-exfoliated two-dimensional 2H-MoS$_2$**